Int. J. Electrochem. Sci., 16 **(2021)** Article Number: 211127, doi: 10.20964/2021.11.08

International Journal of
ELECTROCHEMICAL
SCIENCE
www.electrochemsci.org

Preparation of High-Performance Multifunctional Carbon as Electrode for Supercapacitors using Recycling Scutellaria baicalensis Georgi Extracting Waste

Hongli Gao, Yves Iradukunda, Zhiqian Li, Yaorui Yao,Yang Yang, Guoying Wang, Gaofeng Shi[*]

School of Petrochemical Engineering, Lanzhou University of Technology, Lan gong ping Road, Lanzhou, Gansu, China
[*]E-mail: 1481745684@qq.com

Received: 12 July 2021 / *Accepted:* 27 August 2021 / *Published:* 10 October 2021

Recycling and reusing waste to lessen environmental impact has always been a hot topic in research. The residue of Scutellaria baicalensis Georgi were used in this paper to demonstrate a new process for manufacturing multifunctional carbon compounds. So far, the waste from extracting active compounds from Scutellaria baicalensis Georgi has been used as a raw material, using KOH as an activator and carbonization in a tube furnace at a high temperature to produce a multifunctional carbon material. However, the analysis of Raman, X-ray diffraction and X-ray electron energy spectroscopy, the results depict that the carbon material has been successfully prepared; SEM and BET characterization indicated that the material not only has a large specific surface area (1666.6 cm2/g), but also contains a lot of mesopores and micropores that can be used as excellent adsorption materials and carriers; after optimizing the preparation conditions. As a result of the electrochemical performance analysis, the carbon material has a specific capacitance of 223.6 F/g at 0.5 A/g in a 6 M KOH aqueous solution, demonstrating that it has excellent electrochemical performance and can be used as an alternative material for the preparation of high-performance supercapacitors. The synthesis of multifunctional carbon materials from the residual of Scutellaria baicalensis Georgi extract provides a strong approach to maximizing the value of Scutellaria baicalensis Georgi resources while lowering environmental impact and meeting green energy production needs.

Keywords: Baicalensis; Recycling; Multifunctional Carbon; Reduce environmental burden

1. INTRODUCTION

In recent years, the problem of global warming has intensified, and fossil fuels are not inexhaustible. The search for alternative renewable energy sources has attracted widespread attention from all walks of life around the world[1,2]. In green energy technology, supercapacitors are considered environmentally friendly. As a new type of energy storage device, it has the advantages of

fast charge and discharge process, high power density, good stability, small size, and low price[3,4]. After the research and development of electrode materials by predecessors, there are many kinds of electrode materials, including carbon electrode materials, conductive polymer electrode materials, metal oxide electrode materials, composite electrode materials, etc[5]. Carbon materials with high surface area, such as activated carbon, carbon nanotubes, graphene, etc., are used as electrode materials[6–9].

Porous carbon materials have a good pore structure, which can provide a large specific surface area, have multiple binding sites and high surface reactivity of functional groups, so they have multiple functions and are widely used[10]. It can be used not only as an electrode material, but also as a good adsorbent and photocatalyst carrier [11]. The raw materials for preparing carbon materials mainly come from some non-renewable resources, such as coal and petroleum coke, so their prices are relatively expensive[12]. Using biomass as a raw material can greatly reduce its cost, and it has been introduced to synthesize multifunctional carbon materials[13].

Scutellaria baicalensis contains a lot of natural active molecules, but the active substances will produce a lot of waste after extraction. The common treatment method is to use it as feed or compost. These methods not only waste resources, but also cause environmental pollution[14]. The extensive application of green carbon materials in different fields has been deeply studied[15,16]. In this study, the waste residue after the extraction of active substances from Scutellaria baicalensis Georgi was recycled and reused, which not only reduced the burden on the environment caused by a large amount of waste disposal, but also reduced the waste of resources and improved the utilization rate of Scutellaria baicalensis resources.

2. EXPERIMENTAL

2.1. Reagents and Materials

All the chemical reagents used in the different experiments in this work are of analytical grade.

The deionized water, potassium hydroxide (KOH) Acetylene black, PTFE solution (60%) and hydrochloric acid (HCl) used in this experiment were purchased from Chemical Reagent Co., Ltd. foam nickel (2 cm * 1 cm)

Home-planted Scutellaria baicalensis Georgi

2.2. Equipment

High-speed wall breaking machine, high temperature tube furnace, sand core funnel, vacuum drying oven, porcelain boat, electrochemical workstation

2.3. Eexperimental methods

The scutellaria extract remaining residue is dried, crushed, and passed through a 100-mesh sieve. Select activator, screen carbonization temperature, carbonization time, activator ratio and pre-

carbonization conditions. KOH was selected as the activator. After pre-carbonization at 400°C for 1 hour, 0.5 times the amount of KOH was used for ultrasonic immersion treatment, the tube furnace was set up with a 5°C/min heating program, and the temperature was carbonized at 800°C for 1 hour under the protection of nitrogen.

The carbon material that has been carbonized at 800℃ for 1h is marked as HD, and the carbon material obtained under the optimal conditions is marked as YB.

2.4. Electrochemical test

The electrochemical performance test was performed on the three-electrode CHI660E electrochemical workstation. Mix the carbon material with a mass ratio of 0.8:0.15:0.05, acetylene black, and polytetrafluoroethylene, uniformly coat half of the surface of 1cm×2cm foam nickel, dry at 80°C for 12h (Y11), press 10 trillion Press the tablets for 1 min, weigh the mass, and perform constant current charge and discharge with a current density of 0.5A/g-10 A/g in a three-electrode electrochemical workstation with a saturated calomel electrode as the reference electrode and a platinum plate as the counter electrode (GCD), cyclic voltammetry (CV) and impedance (EIS) testing with sweep speed ranging from 5 mV/s to 100 mV-1. The specific capacitance calculation formula is as follows:

$$\mathrm{Cs} = \frac{\mathrm{I}\Delta\mathrm{t}}{\mathrm{m}\Delta\mathrm{V}}$$

C is the specific capacitance (F/g), I is the discharge current (A), m is the sample mass (g), δt is the discharge time (s) and ΔVis the potential window of discharge (V)[17].

2.5. Structure characterization

The surface morphology and structure of multifunctional carbon materials were analyzed by cold field emission scanning electron microscope (SEM, JSM-6701 fjapan electronic Optics). Using Micromeritics ASAP 2420 surface analyzer, the specific surface area and pore size distribution of the material were calculated through nitrogen adsorption and desorption test analysis. The crystal structure of the material was evaluated using MSA-XD2 powder X-ray diffractometer (diffraction angle scanning range from 5 to 80°). Use a spectrometer (JYHR800, Raman microscope) to measure the Raman spectrum of the material. The surface composition was tested using X-ray photoelectron spectroscopy (XPS, PHI5702, USA).

3. RESULTS AND DISCUSSION

3.1. SEM and TEM

SEM was used to analyze and compare the surface morphology and pore distribution of the porous carbon (HD) from the residue of unactivated Scutellaria baicalensis Georgi and the porous

carbon (YB) after pre-carbonization and KOH activation. It can be seen from Figure 3.7(a) that the surface of the porous carbon of the unactivated Scutellaria baicalensis extract residue is smooth, and there is no obvious carbon skeleton structure. From the SEM image 3.7 (bc) after activation, it can be seen that the sample HD has undergone pretreatment. After carbonization and KOH activation, the relatively smooth surface appears as a loose porous structure, the degree of graphitization is reduced, and the degree of amorphousness is significantly improved, indicating that the pore structure of YB carbon material is obviously distributed, and the surface area of porous carbon is well extended.

TEM further analyzed the surface morphology, amorphous composition, pore structure, etc. of the material, and showed that the material YB has a uniform microstructure. It shows that the YB material has mesopores (2-50nm), which is very important for the movement of the electrolyte[18]. It can be seen from the selected electron diffraction pattern in Figure 1e that clear stripes and planes of (002) and (100) carbon are shown, which indicates that the carbon material has been successfully prepared[19–21].

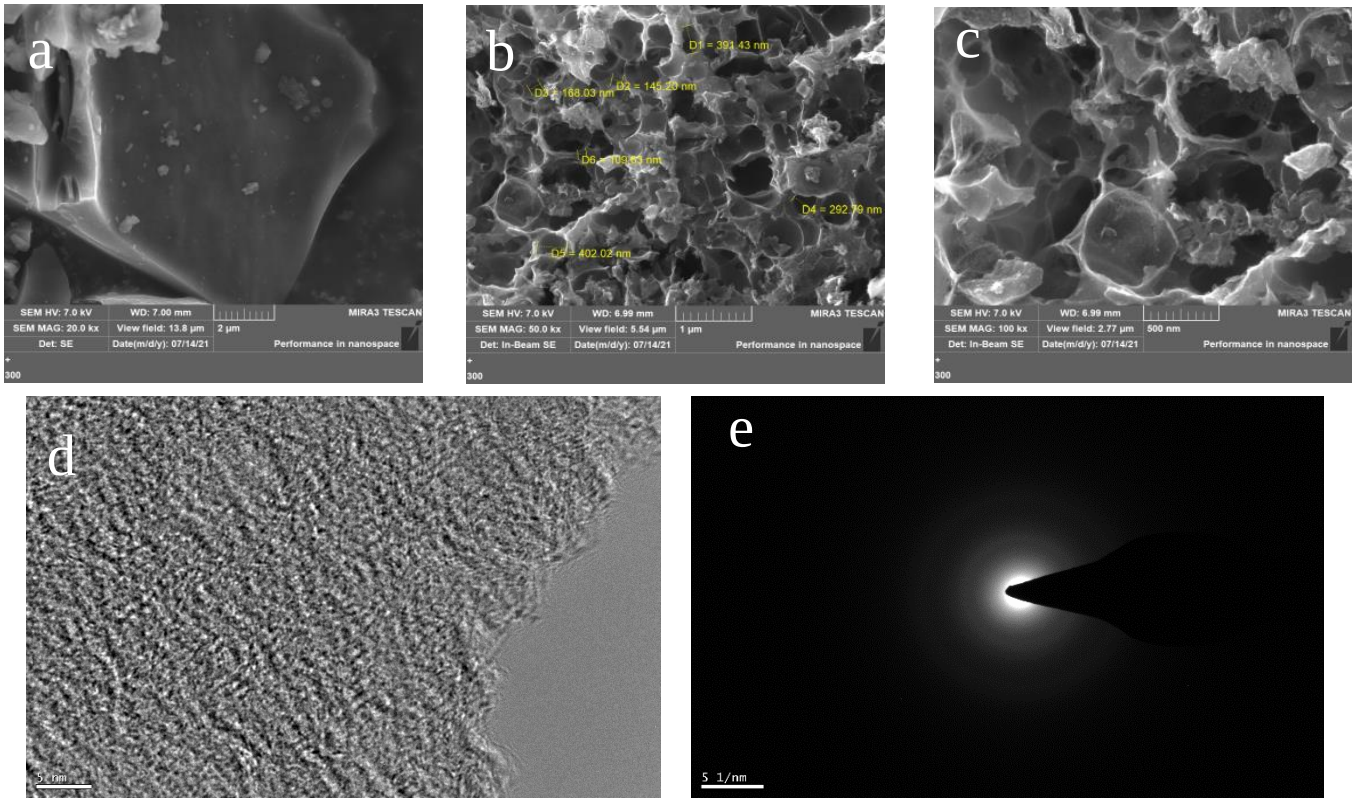

Figure 1. (a)SEM image of HD;(b-c) SEM images of YB;(d) TEM images of YB;(e)the selected area electron diffraction pattern

3.2. XRD and Raman analysis

Raman analysis of materials, as shown in Figure 2 (a), there can be two feature. The G peaks at 1340 cm-1 are respectively corresponding to the G peaks at 1590 cm-1. The D peak represents the defect of atomic lattice, and G peak represents C atomic SP2 hybrid[22]. The intensity ratio (ID / IG)

reflects the softening and graphite level of the material. The Id / Ig values of the D-peaks of the material HD and YB and the g peaks were 0.93 and 0.96, respectively, indicating that the graphite of the material decreased after the addition of KOH activation treatment, which facilitates the rapid transmission of electrolyte ions, thereby enhancing the capacitance of the material. .

The material HD and YB were analyzed using the D / MAX-2400C X-ray diffraction device (XRD). From Fig. 2 (b), two wide feature appear at 23.5 and 43.7, respectively, corresponding to the (002) crystal surface and amorphous carbon of the graphite layer (100), respectively, of the graphite layer (100), respectively, crystal plane[23,24]. As can also be seen from the figure, the material YB is only the diffraction peak of the carbon element, indicating that the material contains less impurities and high purity[25,26].

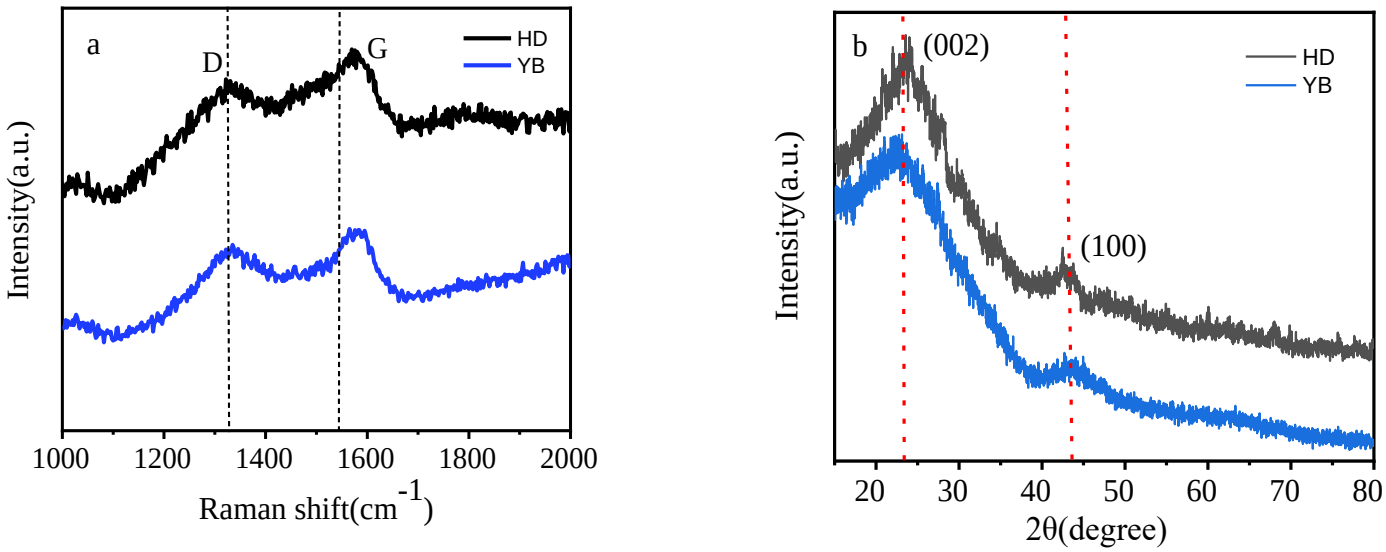

Figure 2. (a) Raman spectra of two samples; (b) XRD patterns of two samples

3.3. XPS analysis

The electronic structure and elements on the surface of YB material were analyzed by X-ray electron spectroscopy. It can be seen from Figure 3a that the material mainly contains two elements, carbon and oxygen, with contents of 88.79% and 11.21% respectively, without N and P elements. The C1s spectrum (3b) and O1s spectrum (3c) were obtained by further peak fitting. The three different peaks in Figure 3b correspond to C=C bond (284.6eV), CO bond (285.5eV) and OC=O bond (289.3eV).)[26–28]. The three different peaks in Figure 3c correspond to C-O bond (531.6eV), C=O bond (532.7eV), O=C-O bond (533.7eV)[29].

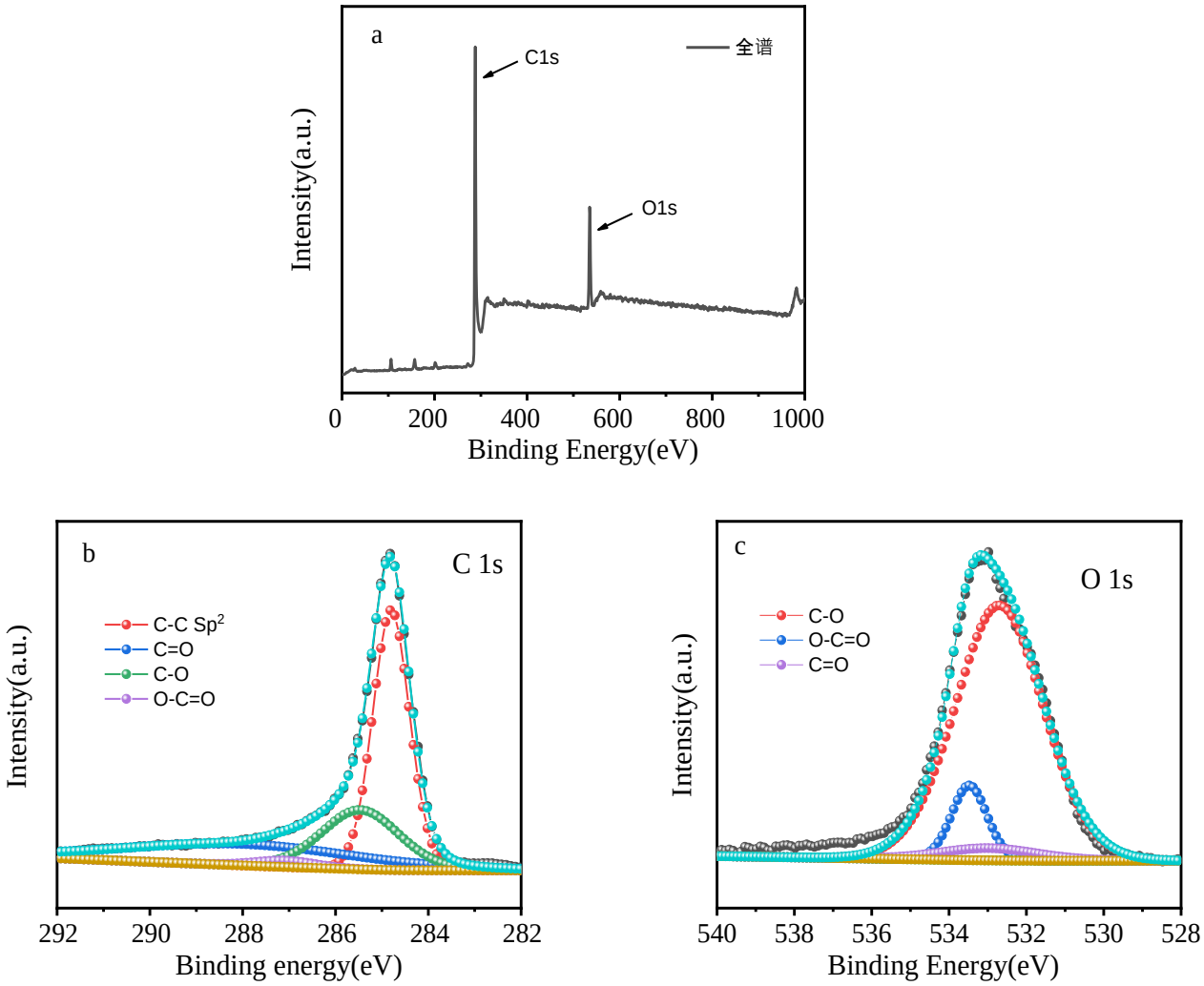

Figure 3. (a) XPS survey spectra of PAC-4, (b-c) C1s and O1s spectra of the PAC-4sample.

3.4 BET analysis

The specific surface area and pore structure of porous carbon are analyzed by nitrogen adsorption and desorption. The adsorption isotherm can be used to analyze whether the material contains micropores (<2nm), mesopores (2-50nm), and macropores (>50nm). Figure (a) shows that the prepared porous carbon material shows type IV adsorption/desorption curve isotherm[30]. It can be seen from the figure that nitrogen adsorption is strong at low relative pressure, while the curve rises gently at medium and high relative pressures, indicating that the material has a microporous structure; when the relative pressure is equal to 0.4, a hysteresis loop indicates the existence of mesopores. Figure (b) is the pore size distribution diagram tested by the BJH method. It can be seen that after screening the activation conditions, the porous carbon microporous and mesoporous structure is significantly improved, and the specific surface area is significantly increased.

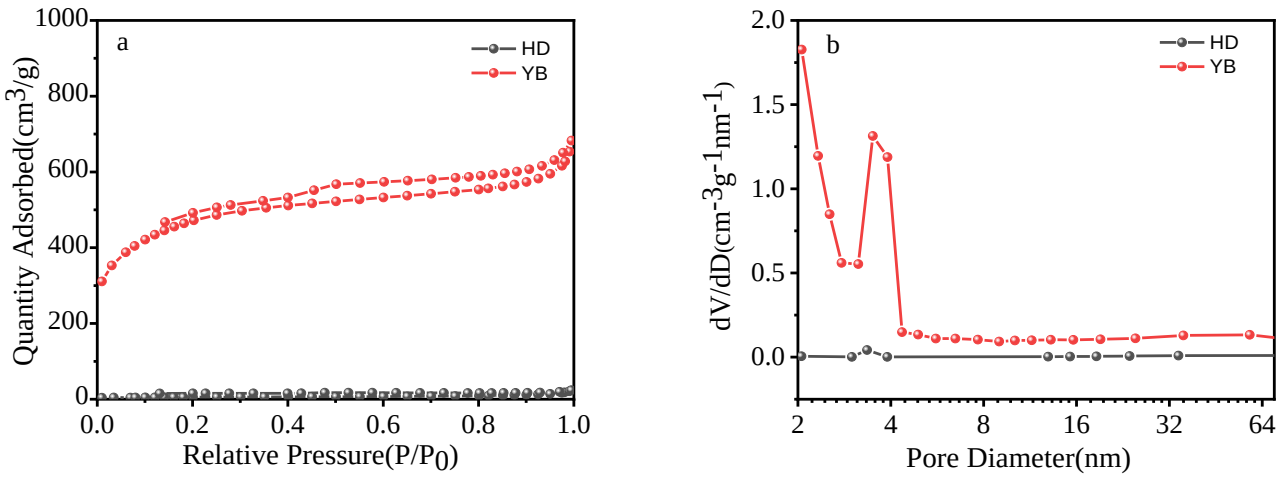

Figure 4. The nitrogen adsorption/desorption isotherm of the sample and Sample method for BJH calculation of pore size distribution.

Table 1. The pore size distribution of porous carbon

Sample	S_{BET} （cm^2/g）	V_t （cm^3/g）	D_{av} （nm）	V_{mic} （cm^3/g）	S_{mic} （cm^2/g）	S_{ext} （cm^2/g）
HD	20.73	0.03	5.04	0.0006	2.67	18.07
YB	1666.6	0.95	2.29	0.26	594.32	1072.28

S_{BET} : BET surface area; V_t: Total pore volume; D_{av}: Average pore dismeter ;V_{mic}： Micropore volume; S_{mic}: Micropore surface area; S_{ext}: External surface area

It can be seen from the table that the specific surface area of the porous carbon is 1666.6 cm^2/g, the total pore volume is 0.95 cm3/g, the micropore volume is 0.26 cm3/g (accounting for 27.37% of the total control volume), and the mesopore volume is 0.69 cm3/g (accounting for 72.63% of the total control volume), indicating that the material is rich in micropores and mesopores.

3.5. Electrochemical performance

In the three-electrode electrochemical performance test system, the materials prepared by adding different proportions of KOH activation were tested, and the constant current charge and discharge curves, cyclic voltammograms and impedance diagrams of the materials were measured as shown in Figure 5. It can be seen from figure (a) that the GCD curve is an equisymmetric triangle, showing excellent electric double layer performance[31]. The mass ratios of the extraction residue and KOH are 1:0, 1:0.5, 1:1, and 1:2. After treatment respectively, the specific capacitances at 1A/g are

22.4F/g, 210.5F/g, 156.8F, respectively. /g, 65.7 F/g. As the amount of KOH increases, the specific capacitance of the material first increases and then decreases. The material obtained by adding 0.5 times the amount of KOH activation treatment has the largest specific capacitance.

Figure (b) is the cyclic voltammogram of materials with different proportions of KOH activation treatment. It can be seen from the figure that the CV diagram of the material without activation treatment is like a triangle, and after KOH treatment is added, the cyclic voltammetry area is significantly increased and the structure is rectangular. 0.5 times the amount of KOH has the largest cyclic volt-ampere area, and there is no redox peak, indicating that the material has good output performance of electric double layer capacitors.

The impedance test was performed on the sample. The result is shown in Figure (c). The impedance curve of the activated carbon material is almost perpendicular to the horizontal axis, and the Weber diffusion curve of the material activated by 0.5 times the amount of KOH is closer to the vertical in the low frequency region. The resistance and charge transfer resistance are smaller, which is also related to the surface structure and pore distribution of the material[24,32,33].

Figure 5(d) shows the capacitance retention of KOH-activated materials with different ratios of current density between 0.5A/g-10 A/g. It can be seen from the figure that the capacitance retention of the material when the activator is 0, 0.5, 1.5, and 2 is added. The rates are respectively 31.25%, 86.59%, 85.44%, 83.71%, and 0.5 times the amount of KOH activation treatment material maintains better capacitance.

It can be seen from Fig. 5(e) that the GCD curve of YB is similar to rectangle under 0.5-10A/g.Figure 5(f) is the cyclic voltammogram of YB at a scan rate of 5-100mV/s. It can be seen from the figure that as the scanning speed increases, the cyclic voltammogram-like rectangularity becomes worse, but at a high scanning rate, the CV curve can still be rectangular-like, indicating that the material has good ion transmission capacity and charge and discharge.performance.

In summary, the electrochemical performance of the carbon material prepared by adding 0.5 times the amount of KOH treatment is more superior.

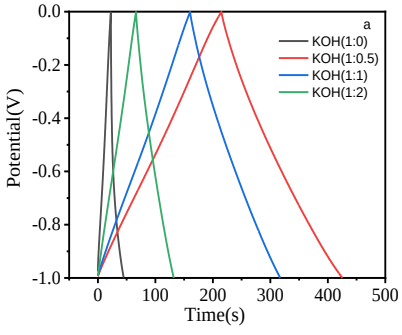

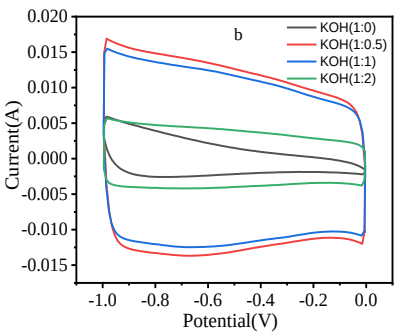

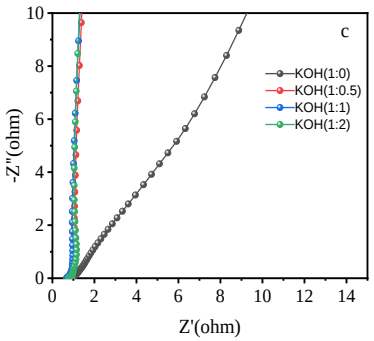

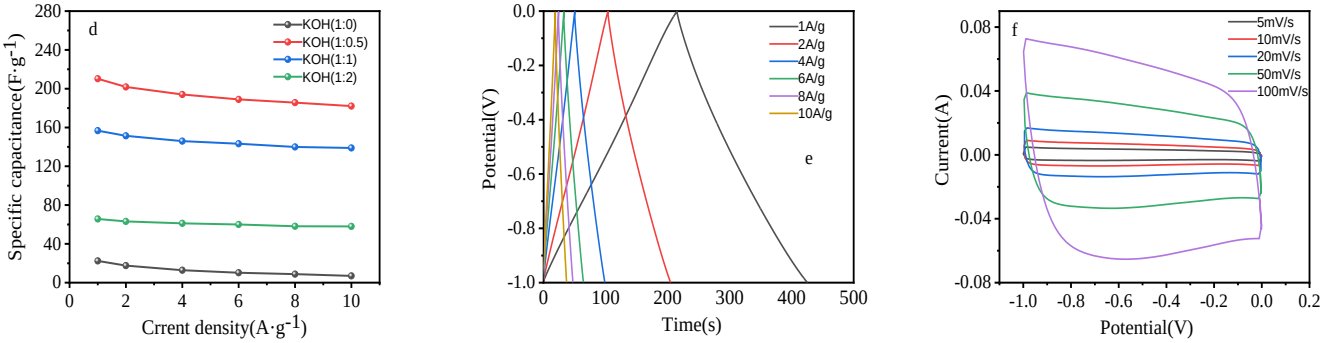

Figure 5. (a)GCD curves of samples at the current density of 1A/g; (b)CV curves of samples at a scan rate of 20mV/s; (c)EIS of samples; (d)specific capacitance of the samples versus various current YB at scan rates ranging from 5 mV/s -100 mV/s.

Table 3. Comparison of electrochemical performance of porous carbon with other different materials

Biomass precursor	Electrolyte	Specific capacity(F/g) (current density)	S_{BET} （cm^2/g）	Reference
Camellia pollen	2M KOH	205(0.5A/g)	526	[34]
Fujimoto bean	6M KOH	219(1A/g)	1159	[35]
Licorice	6M KOH	320(0.5A/g)	2103	[36]
Yellow horn	6M KOH	246.5(1A/g)	1530	[37]
Baicalensis	6M KOH	210.5(1A/g)	1666	This study

4. CONCLUSION

In summary, this study recovered the residue of Scutellaria baicalensis Georgi as a carbon source. By screening the activator and its ratio, and screening the pre-carbonization and carbonization conditions, a multifunctional carbon material with excellent performance was successfully prepared, and the carbon material was finally prepared with a specific surface area as high as 1666.6 cm^2/g, with rich and uniform mesoporous and microporous structure, and good electrochemical performance. It can be used not only as a supercapacitor material, but also as a support or adsorption material.

NOTES

The authors declare no conflicts of interest.

ACKNOWLEDGMENTS

This work was supported by the National Key R & D Program of China (No. 2016YFC0202900), the National Natural Science Foundation of China (No. 21567015, 21407072), the Natural Science Founda tion of Gansu Province (No. 18JR3RA079, 17JR5RA109), the Project of Food and Drug Administratio n of Gansu Province (No. 2018GSFDA014), the Gansu Provincial Party Committee Young Creative T alents (No. Ganzutongzi[2017]121), the Hongliu Science Fund for Distinguished Young Scholars (201 8), and Lanzhou University of technology Hongliu first-class discipline construction program.

References

1. S.H. Kazemi, M. Tabibpour, M.A. Kiani, H. Kazemi, *RSC Adv.*, 6 (2016) 71156–71164.
2. T.M. Gür, *Energy Environ. Sci.*, 11 (2018) 2696–2767.
3. A.G. Pandolfo, A.F. Hollenkamp, *J. Power Sources*, 157 (2006) 11–27.
4. M. Jung, E. Jeong, Y. Kim, Y. Lee, *J. Ind. Eng. Chem.*, 19 (2013) 1315–1319.
5. C. Liu, G. Shi, G. Wang, P. Mishra, S. Jia, X. Jiang, P. Zhang, Y. Dong, Z. Wang, *RSC Adv.*, 9 (2019) 6898–6906.
6. X. Yu, C.J. Hughes, N. Satish, O. Mutlu, S. Devadas, *Proc. Annu. Int. Symp. Microarchitecture, MICRO*, Part F131207 (2017) 1–14.
7. F. Ran, Z. Wang, Y. Yang, Z. Liu, L. Kong, L. Kang, *Electrochim. Acta*, 258 (2017) 405–413.
8. E. Frackowiak, V. Khomenko, K. Jurewicz, K. Lota, F. Béguin, *J. Power Sources*, 153 (2006) 413–418.
9. Y. Yang, L. Zhao, K. Shen, Y. Liu, X. Zhao, Y. Wu, Y. Wang, F. Ran, *J. Power Sources*, 333 (2016) 61–71.
10. H. Sayğili, F. Güzel, *J. Clean. Prod.*, 113 (2016) 995–1004.
11. G. Selvaraju, N.K.A. Bakar, *J. Clean. Prod.*, 141 (2017) 989–999.
12. A.S. Khan, Z. Man, M.A. Bustam, C.F. Kait, A. Nasrullah, Z. Ullah, A. Sarwono, P. Ahamd, N. Muhammad, *J. Clean. Prod.*, 170 (2018) 591–600.
13. Z. Gao, Y. Zhang, N. Song, X. Li, *Mater. Res. Lett.*, 5 (2017) 69–88.
14. G. Wang, Y. Iradukunda, G. Shi, P. Sanga, X. Niu, Z. Wu, *J. Environ. Sci.*, 99 (2021) 324–335.
15. X. Huang, B. Dai, Y. Ren, J. Xu, C. Zhao, *J. Mater. Sci. Mater. Electron.*, 26 (2015) 2584–2588.
16. Y. Wang, *Proc. - 2019 Int. Conf. Robot. Intell. Syst. ICRIS 2019* (2019) 261–264.
17. X. Hao, J. Wang, B. Ding, Y. Wang, Z. Chang, H. Dou, X. Zhang, *J. Power Sources*, 352 (2017) 34–41.
18. Y. Iradukunda, G. Wang, X. Li, G. Shi, Y. Hu, F. Luo, *J. Energy Storage*, 39 (2021) 102577.
19. X.F. Zhang, B. Wang, J. Yu, X.N. Wu, Y.H. Zang, H.C. Gao, P.C. Su, S.Q. Hao, *RSC Adv.*, 8 (2018) 1159–1167.
20. D. Zhang, M. Han, B. Wang, Y. Li, L. Lei, K. Wang, Y. Wang, L. Zhang, H. Feng, *J. Power Sources*, 358 (2017) 112–120.
21. R. Wang, P. Wang, X. Yan, J. Lang, C. Peng, Q. Xue, *ACS Appl Mater Interfaces*, 4 (2012) 5800–5807.
22. X.L. Su, S.H. Li, S. Jiang, Z.K. Peng, X.X. Guan, X.C. Zheng, *Adv. Powder Technol.*, 29 (2018) 2097–2107.
23. C. Bommier, W. Luo, W.-Y. Gao, A. Greaney, S. Ma, X. Ji, Y. Cao, L. Xiao, M.L. Sushko, W. Wang, B. Schwenzer, J. Xiao, Z. Nie, L. V. Saraf, Z. Yang, J. Liu, V. Raju, J. Rains, C. Gates, W. Luo, X. Wang, W.F. Stickle, G.D. Stucky, X. Ji, M.D. Slater, D. Kim, E. Lee, C.S. Johnson, Y. Sun, L. Zhao, H. Pan, X. Lu, L. Gu, Y.-S. Hu, H. Li, M. Armand, Y. Ikuhara, L. Chen, X. Huang, H. Zhu, Z. Jia, Y. Chen, N. Weadock, J. Wan, O. Vaaland, X. Han, T. Li, L. Hu, *Nano Lett.*, 4 (2013) 1870.
24. S. Lei, L. Chen, W. Zhou, P. Deng, Y. Liu, L. Fei, W. Lu, *J. Power Sources*, 379 (2018) 74–83.
25. C. Ma, R. Wang, Z. Xie, H. Zhang, Z. Li, J. Shi, *J. Porous Mater.*, 24 (2017) 1437–1445.
26. D. Zhang, M. Han, Y. Li, J. He, B. Wang, K. Wang, H. Feng, *J. Power Sources*, 372 (2017) 260–269.
27. Y. Zhou, R. Ma, S.L. Candelaria, J. Wang, Q. Liu, E. Uchaker, P. Li, Y. Chen, G. Cao, *J. Power Sources*, 314 (2016) 39–48.
28. J. Zhou, Z. Zhang, W. Xing, J. Yu, G. Han, W. Si, S. Zhuo, *Electrochim. Acta*, 153 (2015) 68–75.
29. H. Chen, Yan-chuan Guo, F. Wang3, G. Wang4, P.Q. 1, 4 , Xuhong Guo 1, *New Carbon Mater.*, 32 (2017) 592–599.

30. H. Lu, W. Dai, M. Zheng, N. Li, G. Ji, J. Cao, *J. Power Sources*, 209 (2012) 243–250.
31. M.F. El-Kady, V. Strong, S. Dubin, R.B. Kaner, *Science*, 335 (2012) 1326–1330.
32. H. Jin, J. Hu, S. Wu, X. Wang, H. Zhang, H. Xu, *J. Power Sources*, 384 (2018) 270–277.
33. W. Li, F. Zhang, Y. Dou, Z. Wu, H. Liu, X. Qian, D. Gu, Y. Xia, B. Tu, D. Zhao, *Adv. Energy Mater.*, 7 (2011) 382–386.
34. C. Lu, J. Li, J.P. Cheng, *J. Power Sources*, 394 (2018) 9–16.
35. G. Shi, Z. Wang, C. Liu, G. Wang, S. Jia, X. Jiang, Y. Dong, Q. Zhang, *Int. J. Electrochem. Sci.*, 14 (2019) 5259–5270.
36. K. Yi, Y. Iradukunda, F. Luo, Y. Hu, X. Li, G. Wang, G. Shi, *Int. J. Electrochem. Sci.*, 16 (2021) 210325.
37. F. Luo, Y. Iradukunda, K. Yi, Y. Hu, X. Li, G. Wang, G. Shi, *Int. J. Electrochem. Sci.*, 16 (2021) 210371.